Applied GIS

ISSN: 1832-5505

Vol-10, Issue-01, 2022

A FLEXIBLE HYDROFOIL PROPELLER SIMULTANEOUSLY LIKE A FISH

Dr. R. Suresh Kumar, Mr. M. Naveenkumar, Mr. S. A. Vasudevan, Mr. V. Prakash

Professor [1], Assistant Professor [2,4], Associate Professor [3]

sureshkumar.r@actechnology.in, mnaveen@actechnology.in, vasudevan@actechnology.in, vprakash@actechnology.in

Department of Mechanical Engineering, Arjun College of Technology, Thamaraikulam, Coimbatore-Pollachi Highway, Coimbatore, Tamilnadu-642 120

ABSTRACT

The hydrofoil is a common option for UAVs because to its remarkable hydrodynamic properties. There is a lot of established study on rigid hydrofoils, but the caudal fin and other flexible hydrofoils have not gotten nearly as much attention as they should. The fish was regarded as the bionic object in this investigation. The kinematics model was then suggested as a means of explaining the fish's swimming action. A fin-peduncle propulsion system was created with a kinematics model to imitate this sine curve motion while swimming. By optimising the propulsion mechanism in Matlab, the fin-peduncle propulsion mechanism's output curve became more in line with the real motion trajectory. In addition, the adjustable articulations' motion phase angles are fine-tuned to boost the propulsion system's efficiency and decrease drag. The last step is to simulate the hydrofoil's fish-like oscillation using a Fluent-based fluid-solid coupling method. It was shown that a fish-like flexible oscillation may be tweaked to generate motion satisfying the same sine law. In comparison to screw propellers, oscillating hydrofoil propellers are much more efficient in propelling, and flexible oscillation outperforms rigid oscillation in this regard without noticeably raising fluid resistance.

Keywords:bionics; flexible hydrofoil; phase angle; hydrodynamic coefficient

INTRODUCTION

When it comes to marine jobs like underwater pipeline construction and equipment maintenance, the Autonomous Underwater Vehicle (AUV) is a lifesaver. Natural development has been aided by marine life for millions of years. Research on AUVs might benefit greatly from the incorporation of bionics. Underwater, fish swam with ease and speed. Dolphins can swim at speeds ranging from three to seven times their own length per second, and their turning radius may be twenty-three to thirty percent of their body length [1]. Robo Tuna, developed at MIT in 1994, was the first fish-like robot; it had a maximum swimming speed of 2 m/s [2]. The media's coverage of the robot that looks like a fish has only grown since then. The PF-300 [3] is a robot that looks like a fish and was created by the Japanese. It has two motors that move its body in tandem. Engineers at Harbin Engineering University designed a lifelike robotic bluefin tuna [4] with a realistic appearance, down to the three-link tail. Du Ruxu's robotic fish is an engineering wonder, with a supple body and a propeller efficiency of up to 65% [5]. Beihang

ISSN: 1832-5505

Vol-10, Issue-01, 2022

University researchers developed SPC, robots that swim like fish, and they've already covered 70.2 km [6]. Numerous numerical studies examining the hydrodynamic characteristics of a hydrofoil in oscillation have also been conducted. To define the conditions under which fish could gain an advantage from enhanced Froude propulsion efficiency, the slender-body hypothesis was put forward for the deformable body [7]. The hydrodynamic characteristics of swimming motion were studied by numerically simulating a three-dimensional flexible fish model [8]. The time-dependent turbulent flows around a Clark-Y hydrofoil were characterised by ridges of the finite-time Lyapunov exponent (FTLE)–described Lagrangian coherent structures (LCS) in this study [9]. When compared to the screw propeller, the fish-fin-shaped flexible oscillating hydrofoil propeller offers superior responsiveness and propulsion efficiency. In this work, we built and optimised a fin-peduncle propulsion system that mimics the way fish swim. In addition, the propulsion system's efficiency is enhanced by adjusting the phase angles of the several articulations that may be moved. The last step is to simulate the hydrofoil's fish-like movement using Fluent and a fluid-solid coupling technique.

PROPULSION MECHANISM

KINEMATICS MODEL

An equation was proposed to characterise the centerline trajectory of the swimming body of a fish based on observations of its swimming [10].

$$h(x_n,t) = H(0.21 - 0.66x_n + 1.1x_n^2 + 0.35x_n^8)sin(2\pi ft) \quad (1)$$

The equation may be paraphrased as follows: n x is the ratio of the body's coordinate value (x) to its length (L), t is the time it takes for the body to move, is its oscillation amplitude, H is its greatest oscillation amplitude at the end of the caudal peduncle, and f is its oscillating frequency. Wang modified the kinematics model after observing the oscillatory motions of the fish body [11]. The simplified equation for the centerline trajectory of the fish body may be expressed as follows, assuming that the maximum oscillation amplitude of the head is one tenth of the body length and that the oscillation amplitude of the barycenter is zero:

$$h(x_n,t) = H(0.1 - 1.3x_n + 2.2x_n^2)sin(2\pi ft) \quad (2)$$

The centerline trajectories of the fish body at different moment are shown in Fig. 1.

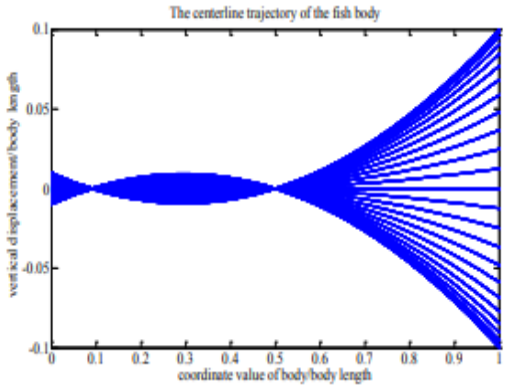

The kinematics equation at the end of the tail can be described as:

$$h(t) = Hsin(2\pi ft) \quad (3)$$

The pitching movement of the caudal fin lags behind its plunging movement, which can be described as:

$$\theta(t) = \theta_{max}sin(2\pi ft + \varphi) \quad (4)$$

the maximum oscillation angle is denoted by θ max, while the phase angle between

ISSN: 1832-5505

Vol-10, Issue-01, 2022

the plunging and pitching movements is represented by ϕ. A fish's caudal fin length (l) and swimming speed (v) are two variables that may be represented graphically. Figure 2 shows how the caudal fin's kinetic coordinate system may be set up.

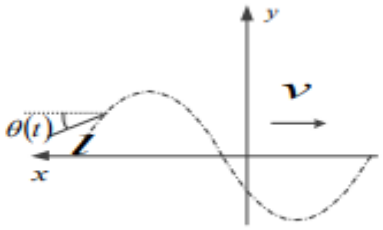

Fig. 2 The kinetic coordinate system for caudal fin

In Figure 2, the caudal fin is shown as a solid line, while its direction of diving movement is shown as a dotted line. The value of the caudal fin's coordinate in the kinetic coordinate at any given moment may be expressed as:

$$x = vt - l\cos[\theta_{max}\sin(2\pi ft + \varphi)] \quad (5)$$

$$y = H\sin(2\pi ft) - l\sin[\theta_{max}\sin(2\pi ft + \varphi)] \quad (6)$$

MECHANISM DESIGN

A kinematics model served as the basis for the design of the propeller mechanism for the fish-like flexible oscillating hydrofoil propeller. Figure 3 shows the schematic of the mechanism.
Figure 3 shows that the servo motor drives member AB as it revolves around A. Member CD, which is linked to member AB via a prismatic joint and a revolute joint, undergoes a transformation from rotation into a sinusoidal reciprocating motion. Revolute joints attach members CD and EF to member DE. Connected to member FG is member EF. It is the job of members CD, DE, EF, and FG to produce the output of the sinusoidal movement. At the very end of member FG is an actuator that, when attached, allows the caudal fin to swing freely behind member FG at a given phase angle.

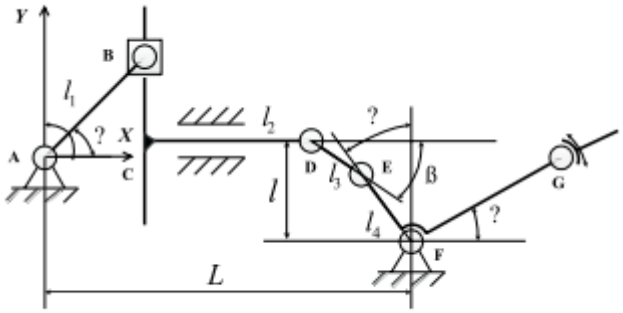

Fig. 3 The mechanism sketch of the propulsion mechanism

The origin is set at point A in the coordinate system shown in Figure 3. In this coordinate system, point F is immobile. Based on the position relations shown in Figure 3, we may derive the following formulas:

$$l_3\sin\beta + l_4\cos\alpha = l \quad (7)$$

$$x_C = l_1\cos\theta \quad (8)$$

$$x_D = l_1\cos\theta + l_2 \quad (9)$$

$$x_E = l_1\cos\theta + l_2 + l_3\cos\beta \quad (10)$$

$$x_F = l_1\cos\theta + l_2 + l_3\cos\beta + l_4\sin\alpha \quad (11)$$

$$l_1\cos\theta + l_2 + \sqrt{l_3^2 - (l - l_4\cos\alpha)^2} + l_4\sin\alpha = L \quad (12)$$

where the coordinate values of C, D, E, and F are represented by Cx, Dx, E, and F x, respectively, and 4l is the length of member AB, member CD, member DE, and member EF. The Y-coordinate of the distance between points D and F is denoted by l. The X-direction distance from A to F is denoted by L. The angles shown in Figure 3 are α, β, and θ. The mechanism schematic served as the basis

ISSN: 1832-5505

Vol-10, Issue-01, 2022

for the propeller model, as seen in Figure 4.

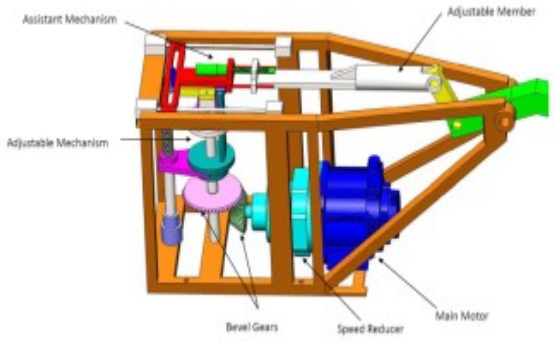

Fig. 4 The propeller model

The length of the member that can be adjusted is changeable. The equilibrium point for the caudal peduncle's diving motion will shift upwards when the adjustable member is shortened and downwards when it is stretched. The fish-like robot may therefore swim in whatever direction it wants by simply adjusting the length of its members.

OPTIMIZATION BASED ON MATLAB

The design of the propulsion mechanism becomes more challenging due to the fact that the length of the mechanism parts influences the diving action of the caudal peduncle. The function approximation approach is now the go-to for designing mechanisms using provided motion laws or trajectories [12]. Optimising a multivariable system, however, is a daunting task. When optimising the design of the mechanism, one may make use of Matlab's many optimisation toolboxes to increase computation efficiency and precision.

As seen in Figure 5, the system for propulsion may be made simpler.

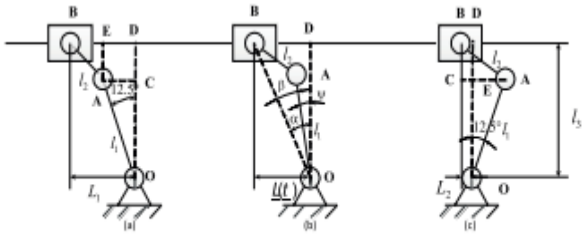

Fig. 5 Mechanism Moment Position

location (b) displays any instant location of the movement, whereas positions (a) and (c) represent the left and right limit positions, respectively. In a sinusoidal reciprocating motion, block B travels. From what we can tell, the oscillation frequency of the diving motion is about 2.1 Hz, and the range of motion is around 25°. This indicates that the OA member has an oscillation range of around 12.5°. Main factors that influence the mechanism's output include the lengths of members OA and AB, the vertical height between points B and O, the movement stroke of block B, and the marks for the position of the two points. The design variables l1, l2, and 31 may be expressed as the following equation:

$$x = [l_1; l_2; l_3]^T \tag{13}$$

As shown in Fig. 5(b), the horizontal distance between point B and point O can be described by L t( ) , as:

$$L(t) = 0.5L\cos 4\pi t + \frac{L_1 + L_2}{2} \tag{14}$$

Where t is the movement time, L1 and L2 are thehorizontal distance of the left limit position and the right position between point B and point O.

As shown in Fig. 5(a) and Fig. 5 (c), L_1 and L_2 can be described as:

ISSN: 1832-5505

Vol-10, Issue-01, 2022

$$L_1 = \sqrt{l_2^2 - (l_3 - l_1 cos12.5°)^2} + l_1 sin12.5° \quad (15)$$

$$L_2 = \sqrt{l_2^2 - (l_3 - l_1 cos12.5°)^2} - l_1 sin12.5° \quad (16)$$

The ideal oscillating law of member OA can be described by Ψ , as:

$$\Psi = 12.5° sin4\pi t \quad (17)$$

To minimize the square of the difference between the mechanism output angle and the ideal output angle, the target function can be described as:

$$F(x) = \sum_{t=0}^{0.25} [\Psi(x) - \Psi]^2 \quad (18)$$

$$\Psi(x) = \alpha(t) - \beta(t) \quad (19$$

where $\alpha(t)$ and $\beta(t)$ can be calculated from ΔOBD and ΔOAB as:

$$\alpha(t) = arccos[\frac{l_3}{\sqrt{l_3^2 + L^2(t)}}] \quad (20$$

$$\beta(t) = arccos\left\{\frac{l_1^2 + [l_3^2 + L^2(t)] - l_2^2}{2l_1\sqrt{l_3^2 + L^2(t)}}\right\} \quad (21$$

Thanks to its sleek design, it offers less resistance while swimming. According to bionics theory, a slim body ratio of 4.5 means that swimming resistance will decrease by 75%. This study stipulates that the robot's fish-like body must not be wider than 0.2 meters in width, and that its length must not exceed 0.9 meters. Also, the robot has to be able to adapt its swimming characteristics to various environments, therefore block B's movement stroke can't be too little if it's going to swim independently. A gearbox angle greater than 40 degrees is required for the mechanism to function properly. The two endpoints of the motion are shown in Figure 6.At the limit position, the gearbox angle should be more than 40° to guarantee excellent gearbox throughout the movement.

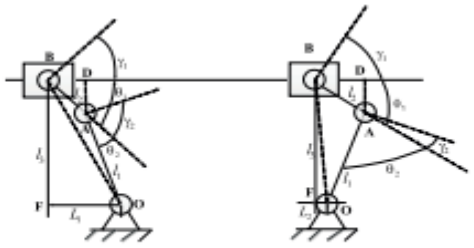

Fig. 6 The transmission angle at the limit position θ_1

In Fig. 6, the constraint conditions of the pressure angle at the limit position can be obtained from ΔADB, as:

$$\frac{l_3 - l_1 cos12.5°}{l_2} \le sin50° \quad (22)$$

In Fig. 6, the constraint conditions of the pressure angle θ_2 at the limit position can be obtained from ΔOAB, as:

$$\frac{L_1^2 + l_3^2 - l_1^2 - l_2^2}{2l_1 l_2} \ge cos50° \quad (23)$$

$$\frac{L_2^2 + l_3^2 - l_1^2 - l_2^2}{2l_1 l_2} \ge cos50° \quad (24)$$

There is a built-in Matlab function called fmincon that may be used to optimise the rod mechanism, which is a nonlinear programming issue. For that reason, the target function was computed at intervals of 0.02s and the totals added together. With 1 l mm = 143.605, 2 l mm = 62.196, and 3 l = 187.8459 mm, the ideal design variables of the solution are [143.605;62.196;187.8459]T x =, as determined by the optimisation. Figure 7 shows the comparison between the ideal output angle and the manufacturing lengths of 1 l mm = 144, l mm = 62, and 3 l mm = 188.

ISSN: 1832-5505

Vol-10, Issue-01, 2022

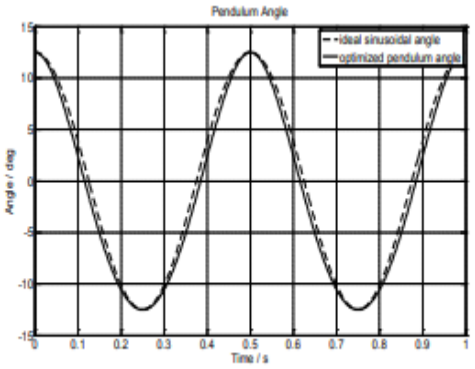

Fig. 7 The output angle of the mechanism and the ideal output angle

Figure 7 shows the developed mechanism's actual output angle and the desired output angle as dashed lines. It is determined that the intended propulsion mechanism has an actual output angle amplitude of 12.5° and that variations occur according to a law of sine, which is comparable to the ideal output angle.

STUDY OF PHASE ANGLE

The forces on the caudal fin were analysed, as shown in Figure 8.

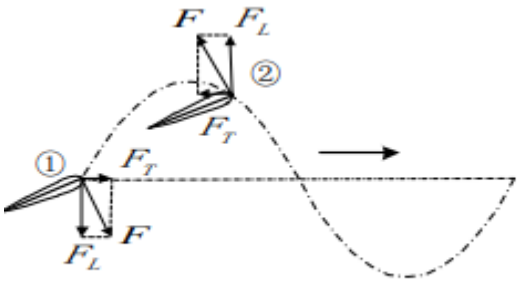

Fig. 8 Analysis of the forces on caudal fin

The positive thrust force, shown as FT in Figure 8, travels forward at. Along with the caudal peduncle, the caudal fin descends at, and the upward force is perpendicular to the fin. The negative thrust force travels in a backwards and forwards manner.

From what we can tell from seeing fish move, there is a straight line between swimming speed and oscillation frequency. In addition, when swimming, the caudal peduncle's oscillation amplitude remains rather constant. The oscillation of the caudal peduncle has an amplitude of around 0.17 to 0.25 times the body length, as pointed out by the biologists. This leads us to the following set of parameters for the robot's movement:

Rate of swimming: v Lm /s ;

The caudal fin has a maximum oscillation range of 0.1 Hz and an oscillation frequency of 2 Hz. The range of the caudal fin's maximum oscillation angle is:

The kinematics simulation is configured with phase differences of 60°, 90°, and 120° between the pitching movement of the caudal fin and the plunging action of the caudal peduncle. From Figures 9 through 11, we can see the caudal fin's oscillations and the swing shaft's motion trajectory.

While the phase difference is 120 degrees, the caudal fin generates the same amount of negative force that a 60-degree phase difference would. At a phase difference of 90 degrees, the caudal fin generates positive thrust during the whole period. A good phase angle for the caudal fin's assault is 90 degrees, which is determined by the phase difference between the fin's diving and pitching movements.

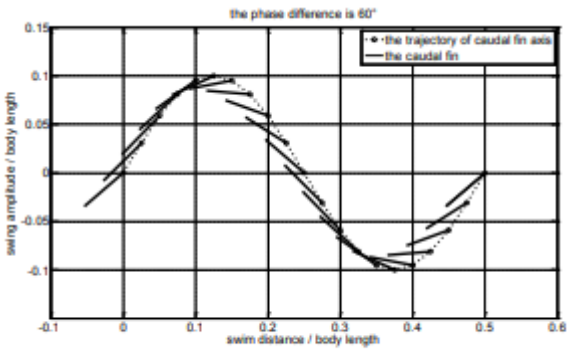

Fig. 9 The phase difference is 60°

ISSN: 1832-5505

Vol-10, Issue-01, 2022

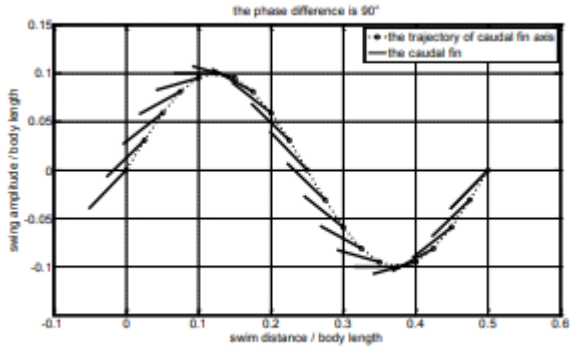

Fig. 10 The phase difference is 90°

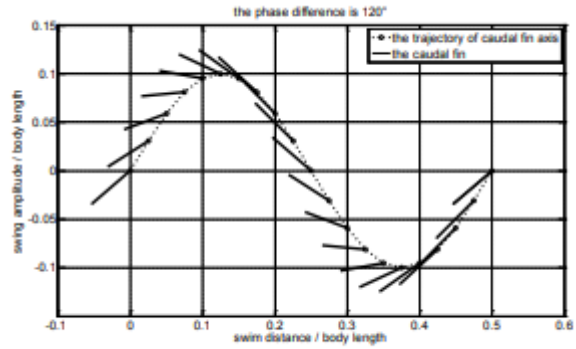

Fig. 11 The phase difference is 135°

HYDRODYNAMIC COEFFICIENTS ANALYSIS

The hydrodynamic coefficients can be defined as:

$$c_d = \frac{F_d}{\frac{1}{2}\rho C_0 v^2} \quad (25)$$

$$c_l = \frac{F_l}{\frac{1}{2}\rho C_0 v^2} \quad (26)$$

$$c_m = \frac{M}{\frac{1}{2}\rho C_0^2 v^2} \quad (27)$$

Equation (d c) represents the drag coefficient, (c1) the lateral force coefficient, (mc) the moment coefficient, (Fd) the drag produced by the flexible oscillating hydrofoil, (Fl) the lateral force produced by the same hydrofoil, (M) the oscillation moment around the fish body's head, (ρ) the fluid density, (C0) the hydrofoil's chord length, and (v) the fluid's flow velocity.

To solve the pressure-velocity coupling equations, the commercial program Fluent's SIMPLE Method was used. To create the flexible oscillation, the UDF, or User Defined Function, was utilised. The fish body and caudal fin in the simulation have an oscillation frequency of 2Hz, an aerofoil of NACA0014, a chord length of 200mm for the fish body and 60mm for the caudal fin, and an oscillating scope of ±45° for the caudal fin. H represents the maximal lateral oscillation amplitude at the end of the fish body in the kinematics model; various values for H indicate varying degrees of flexibility. A greater amplitude of lateral oscillation improves the flexibility. When H is equal to zero, the caudal fin will continue to oscillate normally, but the rest of the fish body will remain stiff.

Under the situation of in-situ fish oscillation, the hydrodynamic properties of a flexible oscillating hydrofoil were studied in calm water. A little water flow velocity is required to run the commercial program Fluent. at keep the flow field from being significantly affected, the velocity was adjusted at 0.01 m/s.

Figure 12 shows the drag coefficient and lateral force coefficient curves over a period in still water, with varying oscillation amplitudes, for a fish body and

ISSN: 1832-5505

Vol-10, Issue-01, 2022

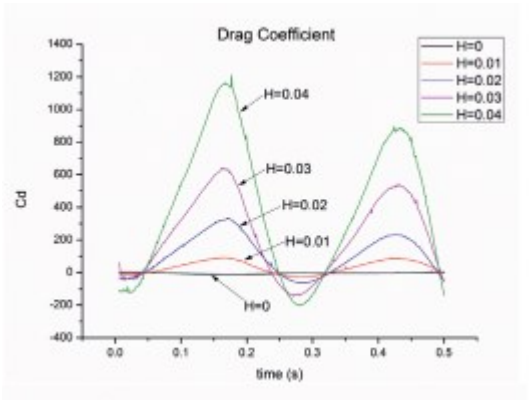

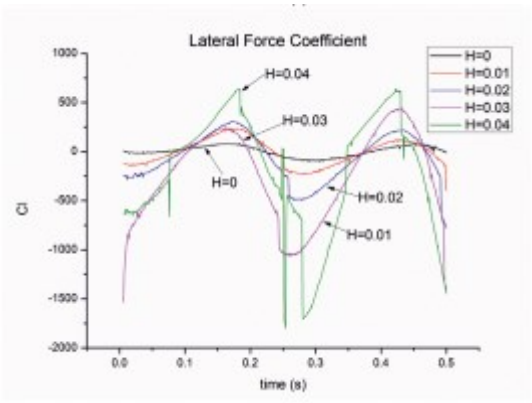

Plots of the fish's drag and lateral force coefficients in calm water (Fig. 12). When the fish body is not oscillating (H = 0), the drag coefficient curves resemble a straight line, indicating that the fish body does not generate thrust force. The bigger the amplitude of the fish's flexible oscillating body, the larger the amplitude of the drag coefficient. An oscillation period in a fish's body has two peaks, and the period of fluctuation in the drag coefficient is half of that. When the numbers are at their highest, it indicates that the fish body is producing the most thrust during the 1/4 and 3/4 periods of its oscillation, respectively. It is possible for the fish to continue its body oscillation in the calm water as the integration value is positive for the whole duration. In the lateral force coefficient curves, we can see that as flexibility improves, the amplitude and fluctuation of the lateral force grow, and that the oscillation-generated lateral force is unstable. Because the fish's body oscillates from side to side along the centre line, the tremendous change happens at the half period of the oscillation. The energy produced by the oscillation is consumed by the lateral force, which in turn increases the swimming instability.

In Fig. 13, we can see the drag coefficient and the lateral force coefficient of the caudal fin as a function of oscillation amplitude in still water throughout that time.

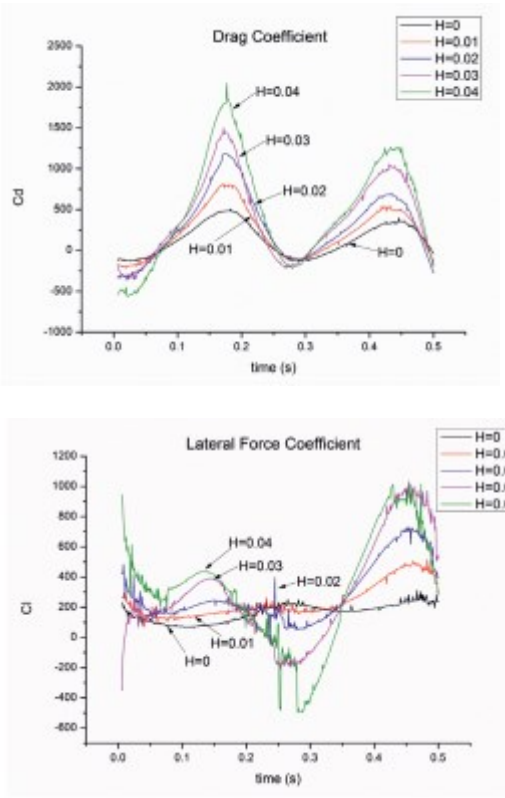

Figure 13: Caudal fin lateral force and drag coefficient curves in calm water Drag coefficient curves reveal that the caudal fin oscillation's change trend mirrors the fish body oscillation's change trend. The caudal fin drag coefficient becomes more pronounced as the fish's flexibility and the amplitude of its oscillations get bigger. The drag coefficient curves for the fish body and caudal fin are compared, and it is observed

ISSN: 1832-5505

Vol-10, Issue-01, 2022

that the caudal fin has a larger drag coefficient value. This suggests that the wake field produced by the oscillation of the fish body enhances the drag coefficient of the caudal fin, in comparison to oscillations without a wake field. Over the full time, the drag coefficient values are almost positive, indicating that the propulsion is clearly affected by the caudal fin oscillation.
It can be observed from the lateral force coefficient curves that the energy produced by the caudal fin oscillation is amplified as the fish's body becomes more flexible and the amplitude of its oscillations increases, all while maintaining the same angle of oscillation. Given that the majority of the lateral force coefficient values are positive and that the integration does not equal zero throughout the oscillation period, it follows that the oscillations of the caudal fin would build up a unidirectional force that opposes swimming. Since the actuator controls the amplitude and phase of the caudal fin oscillation in the growth of the fish-like robot, the unidirectional force should be lowered.

CONCLUSION

In order to guide the construction of the robot fish's propulsion system, our research allowed us to design a kinematics model for its swimming behaviour. To find the ideal length for the pieces of the propulsion system, Matlab's fimincon tool was used. The results demonstrate that the fin-peduncle propulsion system generates motion curves that closely resemble the ideal motion.
Researchers measured how long it took for the caudal fin to pitch and the caudal peduncle to dive. Throughout the whole motion, the thrust mechanism would provide thrust if the phase angle was 90 degrees. The advantages of the articulatory fin-peduncle system are immediately seen, in contrast to the one swinging caudal fin. The period of variation of the moment coefficient is equal to the period of oscillation, whereas the fluctuation periods of the drag coefficient, lateral force coefficient, and moment coefficient are all half of the fish body's oscillation period. A bigger amplitude causes a larger lateral force integration value in a given time period in calm water because the quantity of energy required is proportional to the amplitude of the flexible oscillations.

CONFLICT OF INTEREST

The authors declared that they have no conflicts of interest to this work

ACKNOWLEDGEMENTS

The research was supported by the front and emerging discipline team oriented project of Shandong University “marine resources and utilization of key scientific research”

(project number 2014QY006) and “The Fundamental Research Funds of Shandong University” (2016JC035), hereby thanks.

References

1. Nagai, M. (2002). Thinking fluid dynamics with dolphins. US: IOS Press.

2. Triantafyllou, M. S., and Triantafyllou, G. S. (1995). An efficient swimming machine. Scientific American, 272(3): 64-70.

3. Koichi, H., Tadanori, T., and Kenkichi, T., 2000, “Study on turning performance of a fish robot,” First International Symposium on Aqua Bio-Mechanisms, pp. 287-292.

4. Cheng, W., 2004, “Research on Simulation and Control Technology for Bionic Underwater Vehicle,” Ph.D. thesis, Harbin Engineering University, Harbin, China.

ISSN: 1832-5505

Vol-10, Issue-01, 2022

5. Du, R. X., Li, Z., Kamal, Y. T., Pablo, V. A., 2015, “Robot Fish,” New York: Springer Tracts in Mechanical Engineering.

6. Liang, J. H., Zhang, W. F., Wen, L., Wang, T. M., Liu, and Y. J. (2010). Propulsion and Maneuvering Performances of Two-Joint Biorobotic Autonomous Underwater Behicle SPC-III. Robot, 32(6):726-731.

7. Lighthill, M. J. (1960), Note on the swimming of slender fish, Journal of Fluid Mechanics, Vol.9: 305-317.

8. Leroyer, A., Visonneau, M.(2005), Numerical methods for RANSE simulations of a self-propelled fish-like body, Journal of Fluids and Structures, Vol.20, No.7: 975-991.

9. Zhao, Y., Wang G. Y., Huang, B., Wu, Q., Wang, F. F. (2015), Lagrangian-Based Investigation of Unsteady Vertex Structure Near Trailing Edge of a Hydrofoil, Transactions of Beijing Institute of Technology, Vol.35, No.7: 666-670.

10. Romaneko, E. V. (2002). Fish and dolphin swimming. Bulgaria: Pensoft Publishers.

11. Wang, L., Yu, J. Z., Hu, Y. H., Fan, R. F., Huo, J. Y., and Xie, G. M. (2006). Mechanism design and motion control of robotic dolphin. Acta Scientiarum Naturalium Universitatis Pekinensis, 42(3): 294-301.

12. Wang, W. J. (2006). Optimal design of planar linkage based on Matlab optimization toolbox. Light Industry Machinery, 24(4): 76